Electrohydrodynamics Near Hydrophobic Surfaces

S. R. Maduar,[1,2] A. V. Belyaev,[1,2,3,4] V. Lobaskin,[5] and O. I. Vinogradova[1,2,6,*]
[1]A.N. Frumkin Institute of Physical Chemistry and Electrochemistry, Russian Academy of Sciences, 31 Leninsky Prospect, 119071 Moscow, Russia
[2]Department of Physics, M. V. Lomonosov Moscow State University, 119991 Moscow, Russia
[3]Federal Research and Clinical Center of Pediatric Hematology, Oncology and Immunology, 1 Samora Machel street, 117997 Moscow, Russia
[4]Center for Theoretical Problems of Physicochemical Pharmacology RAS, 38A Leninsky Prospect, 119991 Moscow, Russia
[5]School of Physics and CASL, University College Dublin, Belfield, Dublin 4, Ireland
[6]DWI-Leibniz Institute for Interactive Materials, RWTH Aachen, Forckenbeckstraße 50, 52056 Aachen, Germany
(Received 15 October 2014; published 19 March 2015)

We show that an electro-osmotic flow near the slippery hydrophobic surface depends strongly on the mobility of surface charges, which are balanced by counterions of the electrostatic diffuse layer. For a hydrophobic surface with immobile charges, the fluid transport is considerably amplified by the existence of a hydrodynamic slippage. In contrast, near the hydrophobic surface with mobile adsorbed charges, it is also controlled by an additional electric force, which increases the shear stress at the slipping interface. To account for this, we formulate electrohydrodynamic boundary conditions at the slipping interface, which should be applied to quantify electro-osmotic flows instead of hydrodynamic boundary conditions. Our theoretical predictions are fully supported by dissipative particle dynamics simulations with explicit charges. These results lead to a new interpretation of zeta potential of hydrophobic surfaces.

DOI: 10.1103/PhysRevLett.114.118301 PACS numbers: 47.57.jd, 68.08.-p, 83.50.Lh

The electrostatic diffuse layer (EDL), i.e., the region where the surface charge [1] is balanced by the cloud of counterions, is the central concept in understanding dynamic properties of colloidal systems since it is an origin of numerous electrokinetic effects. This includes electro-osmotic (EO) flow with respect to a charged surface that provides an extremely efficient way to drive and manipulate flows in micro- and nanofluidic devices [2–4]. Most studies of EO assume no-slip hydrodynamic boundary conditions at the surface, which are typical for wettable (hydrophilic) surfaces. In this situation, the *outer* EO velocity u_1 (outside of the *thin* EDL) due to the tangential electric field E_t is given by the Smoluchowski formula,

$$u_1 = -\frac{E_t q_1}{\eta\kappa}, \tag{1}$$

where η is the viscosity of the solution, q_1 is the charge density at the no-slip surface, related to the so-called zeta potential, $\zeta_1 = q_1/\kappa\varepsilon$. Here, ε is the permittivity of the solution, and $\kappa = \lambda_D^{-1}$ is the inverse Debye screening length. Obviously, ζ_1 is equal to the EDL potential.

In practice, however, nonwetting (hydrophobic) materials show hydrodynamic slip, characterized by the slip length b (the distance within the solid at which the flow profile extrapolates to zero) [5]. Some moderate slip, of the order of nanometers, was detected even in weakly hydrophilic systems [6]. For a charge density q_2 at the slipping solid interface, simple arguments show that the outer EO velocity is given by [7,8]

$$u_2 = -\frac{E_t q_2}{\eta\kappa}(1 + b\kappa). \tag{2}$$

The zeta potential was thus interpreted as $\zeta_2 = q_2(1 + b\kappa)/\kappa\varepsilon$. Since, at hydrophobic solids, b can be of the order of tens of nanometers [9–12], for typically nanometric Debye length some small enhancement of the zeta potential and EO flow was observed experimentally [13]. We remark, however, that Eq. (2) fails to predict a realistic ζ_2 of the free interface of bubbles ($b = \infty$) or oil drops [14–16] and, in fact, of systems with large partial slip such as gas sectors of superhydrophobic surfaces [17].

Previous studies assumed that an electric charge associated with slippery surface was *immobile*, which is not justified for bubbles or drops. This is also by no means obvious for hydrophobic solids, because the gas cushion model relates the hydrophobic slip to the formation of a depletion layer at the surface [18]. This idea has received a microscopic foundation in terms of a prewetting transition [19], and was confirmed by recent simulations [20,21]. There is growing evidence that such an interface is weakly charged [22,23]. The existence of surface charges can be caused by ion adsorption [24,25], so that they are laterally *mobile*, and can respond to the external electric field. Indeed, experiments with foam films suggested that an electric field drives charges at the free surface in opposite directions [26], and recent analysis has shown that this could enhance the shear stress [27], but we are unaware of any prior work that has explored what happens in channels with partially slipping hydrophobic walls if adsorbed

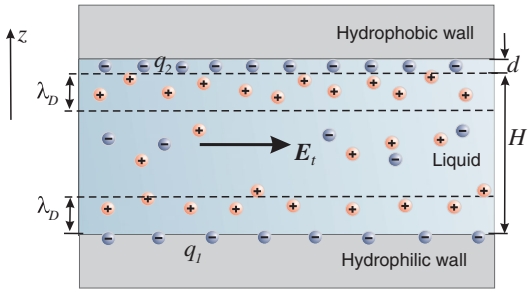

FIG. 1 (color online). Sketch of the system in the case of an asymmetric channel with one no-slip wall. In the case of a symmetric channel, both slippery walls are equal. Fixed surface charges are in the walls; mobile surface charges are adsorbed to the neutral walls. This is important for a definition of H in simulations, but not in the theory, where ions are pointlike, so that d is infinitesimally thin.

charges are mobile. In this Letter, we present some general theoretical arguments and results of dissipative particle dynamics (DPD) simulations, which allow us to quantify an EO flow in such channels. Our analysis leads to a new interpretation of the zeta potential of hydrophobic surfaces.

We consider an EO flow of an aqueous electrolyte solution between two flat walls as sketched in Fig. 1, and define the locus of surfaces at the beginning of EDLs, $z = 0$ and $z = H \gg \lambda_D$, where EO slip velocities and zeta potentials are determined. The hydrophilic surface has a density of charge q_1, and the hydrophobic surface is characterized by the density of charge q_2.

We keep our theory at the mean-field level and treat ions as pointlike. Let us first consider an asymmetric channel with one nonslipping hydrophilic surface ($z = 0 : u = 0$). To describe the fluid velocity at the hydrophobic wall, we suggest a boundary condition, which takes into account that the tangential stress balance represents a combination of both hydrodynamic and Maxwell stress components (see the Supplemental Material [28]),

$$z = H:\ u = b[-\partial_z u + (1-\mu)q_2 E_t/\eta], \tag{3}$$

where parameter μ can vary from 0 for fully mobile charges to 1 in the case of fixed charges. Now we want to compute the velocity profile, which would be expected within a continuous theory when condition (3) is valid.

The fluid flow satisfies Stokes' equations with an electrostatic body force,

$$\eta\nabla^2\boldsymbol{u} = \varepsilon\nabla^2\psi\boldsymbol{E}, \qquad \nabla\cdot\boldsymbol{u} = 0, \tag{4}$$

where the electric field represents a superposition of an external and a created by surface charges fields $\boldsymbol{E} = \boldsymbol{E}_t - \nabla\psi$. The solution of Eq. (4), together with the Poisson-Boltzmann equation and prescribed boundary conditions, in general requires a numerical method. However, in the case of typical for hydrophobic surfaces low surface potentials a solution for $\psi(z)$ can be obtained analytically (see the Supplemental Material [28]). In the thin EDL limit, we then predict an outer EO shear flow,

$$\frac{u(z)}{u_1} = 1 + \frac{z}{b+H}[(1+\mu\kappa b)q_2/q_1 - 1]. \tag{5}$$

The apparent EO slip at the hydrophobic surface is then

$$\frac{u_2}{u_1} = 1 - \frac{1-(1+\mu b\kappa)q_2/q_1}{1+b/H}, \tag{6}$$

which suggests immediately that it is not a unique characteristic of the surface. In contrast, it depends strongly on the second surface of the channel provided b is of the order of H or larger. One striking prediction is that even an uncharged hydrophobic surface, $q_2 = 0$, can induce an apparent EO slip. Another important result is that Eq. (6), even at $\mu = 1$, differs from Eq. (2) derived for a single interface and this suggests that, at $b/H \gg 1$, the EO slip velocity becomes independent on b and saturates to $u_2/u_1 = 1 + \kappa H q_2/q_1$. However, when $\mu = 0$, this large slip limit inevitably leads to $u_2/u_1 = 1$.

Now, the same strategy can be applied for a symmetric hydrophobic channel (with the charge density q_2 and slip length b at both walls), which is also relevant for free soap and foam films that are currently a subject of active research [26,40]. We apply a symmetry condition ($z = H/2 : \partial_z u = 0$) together with Eq. (3) to solve Eq. (4) in the thin EDL limit, and conclude that two situations occur. For a finite slip, we obtain (see the Supplemental Material [28])

$$u_2 = -\frac{E_t q_2}{\eta\kappa}(1+\mu b\kappa). \tag{7}$$

Equation (7) reduces to Eq. (2) when $\mu = 1$ and justifies the use of the Smoluchowski equation when $\mu = 0$. For $b = \infty$ and $\mu = 0$, we predict zero flow rate in the channel with a vanishing at very large κH outer EO velocity [28],

$$u_2 = -\frac{E_t q_2}{\eta\kappa}\frac{2}{\kappa H}, \tag{8}$$

which explains simulation data for this case [41].

In order to assess the validity of the above approach, we employ DPD simulations [42–44] carried out using the open-source package ESPResSo [45] (details are given in the Supplemental Material [28]). We use a simulation cell confined between two impermeable walls always located at $z = 0$ (except the case of a symmetric hydrophobic channel with mobile surface charges, where the lower wall was at $z = -1$) and 14σ, where σ sets the length scale. The value of $\kappa = (8\pi\ell_B c_0)^{1/2}$ with Bjerrum length $\ell_B = e^2/4\pi\varepsilon k_B T$ was determined by using the concentration, $c_0 \simeq 5\times 10^{-2}\sigma^{-3}$, outside EDLs, which gives $\kappa^{-1} = 1 - 1.2\sigma$ and provides large κH. We set up b from 0 to ∞ at the walls by using a tunable slip method [28,46].

Immobile surface charges are implemented by randomly placing discrete unit charges $q_s e$ in the no-slip hydrophilic

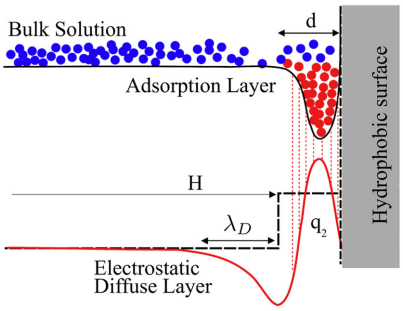

FIG. 2 (color online). Top: Lennard-Jones adsorption potential applied in simulations. Bottom: a concentration profile of adsorbed ions and the model with homogeneous charge distribution inside the adsorbed layer.

walls, to provide homogeneous $q_1 = 0.15 q_s e/\sigma^2$. We adjusted $4\pi \ell_B q_1/\kappa < 1$ to ensure the weak-charge behavior. Fixed charges of a density q_2 at the hydrophobic wall are created similarly.

The mobile charges are modeled by applying an effective interfacial potential, which leads to selective adsorption of one type of ion to an electroneutral hydrophobic wall. Namely, we set Lennard-Jones (LJ) potential between negative ions and the hydrophobic wall (see Fig 2), since it qualitatively reproduces the potentials of mean force for surface active ions [47]. The density of adsorbed charge q_2 can be regulated by the strength of the LJ potential. The ratio q_2/q_1 was varied from 1 ± 0.03 to 3 ± 0.1 by setting different values of q_1 at the no-slip (hydrophilic) surface. Fixed in such a way, adsorbed charges are confined in a layer of thickness d being in thermodynamic equilibrium with the bulk electrolyte solution and respond to E_t. The thickness of the adsorbed layer, $d \simeq \sigma$, is determined from the simulation data (see the Supplemental Material [28]), and the locus of surfaces was at $z \simeq 13\sigma$ or $z = 0$.

We begin by studying an asymmetric channel, where a variety of situations occurs depending on the parameters of the surfaces. Fluid velocity profiles $u(z)$ were first simulated with $q_2/q_1 = 1$, $\kappa H = 12$, and $b/H = 1.2$, by setting mobile ($\mu = 0$) and immobile ($\mu = 1$) charges at the slipping surface. The results are shown in Fig. 3(a). Also included are the data obtained for a channel with two hydrophilic walls ($b = 0$). A general conclusion from this plot is that the simulation results are in excellent agreement with predictions of mean-field theory, confirming the validity of a continuum description and the electrohydrodynamic boundary condition, Eq. (3). For a hydrophilic channel, we observe a classical behavior, where the *inner* fluid velocity in the EDL increases from zero on the surfaces with high gradients to form an outer plug EO flow in the electroneutral center. A hydrophobic slippage strongly amplifies the velocity if surface charges are immobile with an outer shear flow, perfectly described by Eq. (5). The slipping surface with mobile charges generates a plug profile in the center, and neither outer

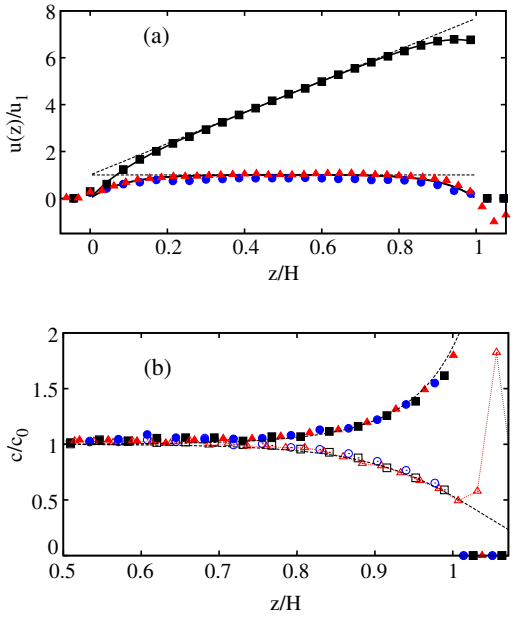

FIG. 3 (color online). (a) Fluid velocity profiles simulated at $q_2/q_1 = 1$ and $\kappa H = 12$ (symbols). Circles correspond to a hydrophilic channel; squares and triangles represent a channel with a hydrophobic surface, $b/H = 1.2$, with $\mu = 1$ and 0. Solid curves show solutions of linearized Eq. (4); dotted lines are predictions of Eq. (5). (b) Corresponding cation (filled symbols) and anion (open symbols) profiles obtained in simulations with the theoretical expectations (dotted curves).

nor inner EO velocities show a manifestation of the hydrodynamic slip. Simulation data show that this is, however, accompanied by some negative flow in the adsorbed layer. We finally note that simulated ion density profiles are superimposed in all cases, as seen in Fig. 3(b). This confirms that the EO slip near hydrophobic surfaces no longer reflects the sole EDL potential.

To explore flow behavior near a hydrophobic surface with mobile charges in more detail, we continue with varying the ratio q_2/q_1 from 0 to 3 at fixed $b/H = 1.2$. The simulation results and theoretical predictions are given in Fig. 4 and are again in a good agreement (since the flow in the adsorbed layer is qualitatively the same as in Fig. 3(a), we do not show it here and below). We see that an apparent

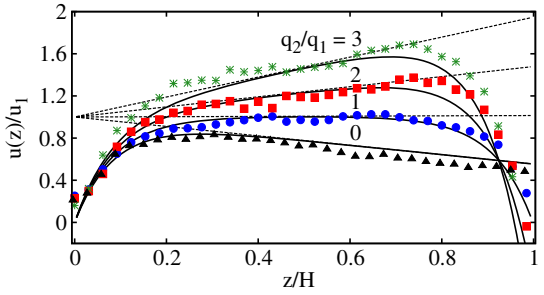

FIG. 4 (color online). Fluid velocity profiles simulated at $\kappa H = 12$, $b/H = 1.2$, $q_2/q_1 = 0, 1, 2, 3$, and $\mu = 0$. Solid curves show theoretical results; dotted lines are predictions of Eq. (5).

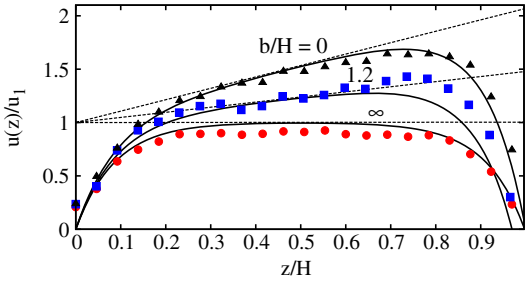

FIG. 5 (color online). Fluid velocity profiles simulated at $\kappa H = 12$, $q_2/q_1 = 2$, and $\mu = 0$ (symbols). From top to bottom, $b/H = 0$, 1.2, and ∞. Solid curves show theoretical results; dotted lines are predictions of Eq. (5).

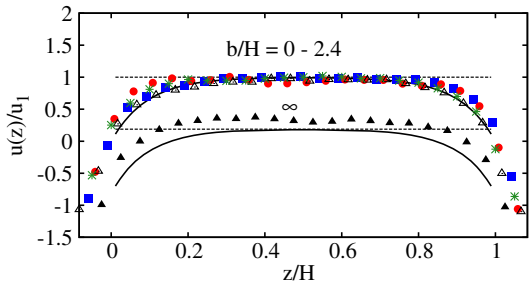

FIG. 6 (color online). Fluid velocity profiles in a symmetric channel simulated at $\kappa H = 11$ and $\mu = 0$ (symbols). Upper curves were simulated at $b/H = 0$, 0.08, 1.3, and 2.4; bottom curve corresponds to $b/H = \infty$. Solid curves show theoretical results; upper dotted lines are predictions of Eq. (7); and lower dotted lines are predictions of Eq. (8).

EO slip u_2 at the hydrophobic surface increases with q_2/q_1, but a variety of physically different situations occurs depending on the value of this ratio. An uncharged hydrophobic surface induces an EO slip, and we see a manifestation of an outer shear flow. As discussed above, in the case of symmetric charges $q_2/q_1 = 1$, we see no indication of a hydrodynamic slip. Finally, for larger q_2/q_1, we again observe an outer shear flow. These observations are well described by Eq. (5). This equation also suggests that if $q_2/q_1 < 1$, the hydrodynamic slippage amplifies u_2 as compared to expected values for a hydrophilic surface, where $u_2 = u_1 q_2/q_1$, but when $q_2/q_1 > 1$ hydrodynamic slip inhibits the apparent EO slip. A key remark is that this amplification or inhibition is no longer dependent on the equilibrium properties of the EDL, but note that a rich outer EO behavior is accompanied by the unusual flow within the EDL. A charged hydrophobic surface actively participates in the flow-driving mechanism since it reacts electrostatically to the field by inducing a forward or backward inner EO flow.

We now illustrate the influence of a hydrodynamic slip on EO flow in the case of $\mu = 0$ (Fig. 5). According to Eq. (6), with the charge ratio $q_2/q_1 = 2$, the apparent EO slip should be inhibited compared to a hydrophilic case, which is fully confirmed by our results. In the case of $b/H = O(1)$, we observe a decrease in the outer shear EO flow and a corresponding apparent EO slip at the hydrophobic surface. However, in the limit of $b = \infty$ (a wetting film), we observe the plug outer flow (also reported in Ref. [27]), which reflects the EDL dynamics, where an electrostatically active interface induces the strong inner flow opposite to the field.

Let us now turn to the EO properties of a symmetric channel with $\mu = 0$ and plot in Fig. 6 the simulated EO velocities (related to u_1 expected in the no-slip case with $q_1 = q_2$) for several values of the slip length. We see that outer and inner EO flows simulated at several finite b values coincide with the Smoluchowski profile as predicted by Eq. (7), which is accompanied by the backward flow in the adsorbed layer. We have also explored what happens when $b = \infty$, and generally confirm a much smaller magnitude of a plug outer flow, also observed in Ref. [41].

Finally, we can interpret a zeta potential of a hydrophobic surface, which is naturally defined as $\zeta_2 = -u_2\eta/E_t\varepsilon$. In a thick asymmetric channel, it is therefore $\zeta_2/\zeta_1 = u_2/u_1$, described by Eq. (6). However, if $b/H \ll 1$, Eq. (6) reduces to

$$\zeta_2 = \frac{q_2(1+\mu\kappa b)}{\kappa\varepsilon}, \tag{9}$$

and zeta potential becomes a characteristic of a hydrophobic surface solely. Equation (9) is relevant for the understanding of highly debated zeta-potential measurements on free interfaces of (not confined) bubbles and oil drops [14–16]. Equation (7) implies that a zeta potential of a hydrophobic surface in a thick symmetric channel is also given by Eq. (9), except the case $b = \infty$ and $\mu = 0$, where zeta potential becomes $\zeta_2 = 2q_2/\epsilon\kappa^2 H \simeq 0$.

In conclusion, we have formulated an electrohydrodynamic slip boundary condition and demonstrated that both confinement and mobility of surface charges have a dramatic effect on the hydrodynamic properties of the EDL and EO flow. Simple analytical formulas for the apparent EO slip and zeta potential at the hydrophobic surface have been suggested, which resolve a number of paradoxes and confusions in the literature. Our results obtained for cases of immobile and fully mobile charges give rigorous upper and lower bounds on an EO slip for arbitrary hydrophobic surfaces given only the surface charge or potential and (any) slip lengths. These bounds constrain the attainable zeta potential, and provide guidance for experimental measurements of μ, which in some real systems could be confined in the interval from 0 to 1. Our study may be immediately extended to the challenging case of $\kappa H = O(1)$ and smaller [3,4], where the outer EO is absent. Another fruitful direction could be to apply our results to revisit calculations of an EO flow past superhydrophobic surfaces [48–50].

This research was partly supported by the Russian Foundation for Basic Research (Grant No. 12-03-00916) and by the DFG through SFB 985. The simulations were carried out using computational resources of the Supercomputing Center of the M. V. Lomonosov Moscow State University.

*Corresponding author.
oivinograd@yahoo.com

[1] In experimental systems, such a surface charge is normally not intrinsic, and is at a (few Å) layer of adsorbed (nondiffuse) counterions but note that in some specific cases the picture can be more complex [51].
[2] T. M. Squires and S. R. Quake, Rev. Mod. Phys. **77**, 977 (2005).
[3] P. B. Schoch, J. Han, and P. Renaud, Rev. Mod. Phys. **80**, 839 (2008).
[4] J. C. T. Eijkel and A. van den Berg, Microfluid. Nanofluid. **1**, 249 (2005).
[5] O. I. Vinogradova, Int. J. Miner. Process. **56**, 31 (1999).
[6] L. Bocquet and E. Charlaix, Chem. Soc. Rev. **39**, 1073 (2010).
[7] V. M. Muller, I. P. Sergeeva, V. D. Sobolev, and N. V. Churaev, Colloid J. USSR **48**, 606 (1986).
[8] L. Joly, C. Ybert, E. Trizac, and L. Bocquet, Phys. Rev. Lett. **93**, 257805 (2004).
[9] O. I. Vinogradova and G. E. Yakubov, Langmuir **19**, 1227 (2003).
[10] C. Cottin-Bizonne, B. Cross, A. Steinberger, and E. Charlaix, Phys. Rev. Lett. **94**, 056102 (2005).
[11] L. Joly, C. Ybert, and L. Bocquet, Phys. Rev. Lett. **96**, 046101 (2006).
[12] O. I. Vinogradova, K. Koynov, A. Best, and F. Feuillebois, Phys. Rev. Lett. **102**, 118302 (2009).
[13] C. I. Bouzigues, P. Tabeling, and L. Bocquet, Phys. Rev. Lett. **101**, 114503 (2008).
[14] P. Creux, J. Lachaise, A. Graciaa, J. K. Beattie, and A. M. Djerdjev, J. Phys. Chem. B **113**, 14146 (2009).
[15] K. G. Marinova, R. G. Alargova, N. D. Denkov, O. D. Velev, D. N. Petsev, I. B. Ivanov, and R. P. Borwankar, Langmuir **12**, 2045 (1996).
[16] M. Takahashi, J. Phys. Chem. B **109**, 21858 (2005).
[17] T. V. Nizkaya, E. S. Asmolov, and O. I. Vinogradova, Phys. Rev. E **90**, 043017 (2014).
[18] O. I. Vinogradova, Langmuir **11**, 2213 (1995).
[19] D. Andrienko, B. Dünweg, and O. I. Vinogradova, J. Chem. Phys. **119**, 13106 (2003).
[20] S. M. Dammer and D. Lohse, Phys. Rev. Lett. **96**, 206101 (2006).
[21] C. Sendner, D. Horinek, L. Bocquet, and R. Netz, Langmuir **25**, 10768 (2009).
[22] V. Tandon, S. K. Bhagavatula, W. C. Nelson, and B. J. Kirby, Electrophoresis **29**, 1092 (2008).
[23] R. A. Pushkarova and R. G. H. Horn, Langmuir **24**, 8726 (2008).
[24] D. J. Tobias, A. C. Stern, M. D. Baer, Y. Levin, and C. J. Mundy, Annu. Rev. Phys. Chem. **64**, 339 (2013).
[25] D. M. Huang, C. Cottin-Bizonne, C. Ybert, and L. Bocquet, Phys. Rev. Lett. **98**, 177801 (2007).
[26] O. Bonhomme, O. Liot, A. L. Biance, and L. Bocquet, Phys. Rev. Lett. **110**, 054502 (2013).
[27] W. Choi, A. Sharma, S. Qian, G. Lim, and S. W. Joo, J. Colloid Interface Sci. **347**, 153 (2010).
[28] See Supplemental Material at http://link.aps.org/supplemental/10.1103/PhysRevLett.114.118301 for a derivation of Eqs. (3), (5), (6), and (7), and details of simulations. The Supplemental Material includes Refs. [13,18,22,23,29–39,42,43,46].
[29] D. Exerowa, N. V. Churaev, T. Kolarov, N. E. Esipova, N. Panchev, and Z. M. Zorin, Adv. Colloid Interface Sci. **104**, 1 (2003).
[30] H. K. Christenson and P. M. Claesson, Adv. Colloid Interface Sci. **91**, 391 (2001).
[31] J. D. Weeks, D. Chandler, and H. C. Andersen, J. Chem. Phys. **54**, 5237 (1971).
[32] J. Smiatek, M. Sega, C. Holm, U. D. Schiller, and F. Schmid, J. Chem. Phys. **130**, 244702 (2009).
[33] J. Zhou, A. V. Belyaev, F. Schmid, and O. I. Vinogradova, J. Chem. Phys. **136**, 194706 (2012).
[34] E. S. Asmolov, J. Zhou, F. Schmid, and O. I. Vinogradova, Phys. Rev. E **88**, 023004 (2013).
[35] R. W. Hockney and J. W. Eastwood, *Computer simulation using particles* (Taylor & Francis, London, 1989).
[36] M. Deserno and C. Holm, J. Chem. Phys. **109**, 7678 (1998).
[37] M. Deserno and C. Holm, J. Chem. Phys. **109**, 7694 (1998).
[38] A. Arnold and C. Holm, in *Advanced Computer Simulation Approaches for Soft Matter Sciences II*, edited by C. Holm and K. Kremer, Advances in Polymer Science Vol. 185 (Springer, Berlin, 2005), pp. 59–109.
[39] A. Arnold, J. de Joannis, and C. Holm, J. Chem. Phys. **117**, 2496 (2002).
[40] L. Joly, F. Detcheverry, and A. L. Biance, Phys. Rev. Lett. **113**, 088301 (2014).
[41] D. M. Huang, C. Cottin-Bizonne, C. Ybert, and L. Bocquet, Langmuir **24**, 1442 (2008).
[42] P. J. Hoogerbrugge and J. M. V. A. Koelman, Europhys. Lett. **19**, 155 (1992).
[43] P. Español and P. Warren, Europhys. Lett. **30**, 191 (1995).
[44] R. D. Groot and P. B. Warren, J. Chem. Phys. **107**, 4423 (1997).
[45] H. Limbach, A. Arnold, B. Mann, and C. Holm, Comput. Phys. Commun. **174**, 704 (2006).
[46] J. Smiatek, M. Allen, and F. Schmid, Eur. Phys. J. E **26**, 115 (2008).
[47] R. R. Netz and D. Horinek, Annu. Rev. Phys. Chem. **63**, 401 (2012).
[48] A. V. Belyaev and O. I. Vinogradova, Phys. Rev. Lett. **107**, 098301 (2011).
[49] T. M. Squires, Phys. Fluids **20**, 092105 (2008).
[50] S. S. Bahga, O. I. Vinogradova, and M. Z. Bazant, J. Fluid Mech. **644**, 245 (2010).
[51] A. V. Delgado, F. Gonzalez-Caballero, R. J. Hunter, L. K. Koopal, and J. Lyklema, J. Colloid Interface Sci. **309**, 194 (2007).